A Single Gene Target of an ETS-Family Transcription Factor Determines Neuronal CO_2-Chemosensitivity

Julia P. Brandt[1], Sonya Aziz-Zaman[1◊], Vaida Juozaityte[2◊], Luis A. Martinez-Velazquez[1], Jakob Gramstrup Petersen[2], Roger Pocock[2]*, Niels Ringstad[1]*

1 The Helen L. and Martin S. Kimmel Center for Biology and Medicine at the Skirball Institute of Biomolecular Medicine, Molecular Neurobiology Program, and Department of Cell Biology, NYU Langone Medical Center, New York, New York, United States of America, **2** Biotech Research and Innovation Centre (BRIC), University of Copenhagen, Copenhagen, Denmark

Abstract

Many animals possess neurons specialized for the detection of carbon dioxide (CO_2), which acts as a cue to elicit behavioral responses and is also an internally generated product of respiration that regulates animal physiology. In many organisms how such neurons detect CO_2 is poorly understood. We report here a mechanism that endows *C. elegans* neurons with the ability to detect CO_2. The ETS-5 transcription factor is necessary for the specification of CO_2-sensing BAG neurons. Expression of a single ETS-5 target gene, *gcy-9*, which encodes a receptor-type guanylate cyclase, is sufficient to bypass a requirement for *ets-5* in CO_2-detection and transforms neurons into CO_2-sensing neurons. Because ETS-5 and GCY-9 are members of gene families that are conserved between nematodes and vertebrates, a similar mechanism might act in the specification of CO_2-sensing neurons in other phyla.

Introduction

CO_2-chemosensitive neurons are found in many animals. In vertebrates, CO_2-sensing neurons are critical regulators of respiration [1]. Their dysfunction is proposed to underlie disorders such as sudden infant death syndrome [2] and congenital hypoventilation syndrome [3]. CO_2 is also sensed by animals as an ethologically relevant environmental cue. For example, insects detect CO_2 in the contexts of host- and mate-finding and as an aversive odorant [4,5], and the rodent olfactory system contains neurons that can be activated by low concentrations of CO_2 [6,7]. Studies of the insect olfactory system have identified odorant receptors that mediate CO_2 sensation, indicating that CO_2 can act through cellular and molecular systems dedicated to its detection [4,8,9]. The molecular mechanisms that mediate CO_2 sensing by insect olfactory neurons are, however, unique to insects. How neurons of other organisms detect CO_2 is poorly understood.

To control internal concentrations of respiratory gases, the microscopic nematode *C. elegans* navigates to environments with preferred concentrations of oxygen and CO_2 [10,11,12,13,14,15]. Two anterior sensory neurons, the BAG neurons, detect environmental CO_2 and mediate a CO_2-avoidance behavior [15,16,17]. CO_2-sensing by BAG neurons requires cyclic nucleotide signaling; mutants that lack either TAX-2 or TAX-4 subunits of a cyclic nucleotide-gated ion channel are defective in behavioral and physiological responses to CO_2 [16,17], as are mutants that lack the receptor-type guanylate cyclase GCY-9 [17]. Because CO_2 activates the BAG neurons of *C. elegans* through a specific molecular pathway, their study offers the opportunity to understand the molecular basis of neuronal CO_2-sensing.

ETS-5, an ETS-domain-containing transcription factor, was recently shown to regulate expression of many BAG-neuron-specific genes [18]. Whether ETS-5 is required for BAG-neuron responses to CO_2, and, if so, how ETS-5 confers CO_2-chemosensitivity to BAG neurons is unknown. We show here that *ets-5* mutants have defects in CO_2 sensory transduction, and that ETS-5 directly interacts *in vitro* and *in vivo* with elements in the promoter of *gcy-9*, which encodes a critical component of the CO_2 sensory transduction pathway. Strikingly, the requirement for ETS-5 in CO_2 sensing can be bypassed by forced expression of *gcy-9*. These data indicate that a mechanism by which ETS-5 specifies CO_2 chemosensitivity of BAG neurons is by direct regulation of the expression of GCY-9. GCY-9 in turn is sufficient to mediate neuronal responses to CO_2 and likely encodes a receptor for CO_2 or a CO_2 metabolite.

Results

One of ten ETS-family transcription factors encoded by the *C. elegans* genome is required for the specification of CO_2-sensing BAG neurons

To identify factors that specify BAG neurons, we analyzed promoters of genes that are expressed by BAG neurons. We hypothesized that identification of cis-regulatory elements required for expression of these terminal differentiation genes in BAG neurons would enable us to identify trans-acting factors required

for BAG neuron differentiation. First we looked at the promoter of the BAG-neuron-specific neuropeptide gene *flp-17*. We dissected a 1460 bp *flp-17* promoter and found that a 138 bp promoter fragment was sufficient to drive expression in BAG neurons (Fig. S1). We noted that this minimal promoter contains three copies of a sequence motif predicted to bind ETS-family transcription factors. We then tested whether a promoter containing a single ETS-binding site is sufficient to drive gene expression in the BAG neurons. We observed that a 31 bp sequence containing a single ETS-binding site drove expression of a reporter transgene specifically in BAG neurons (Fig. 1A). These data indicated that one or more ETS-family transcription factors function to control BAG-cell fate specification.

Which of the ten ETS-family transcription factors encoded by the *C. elegans* genome regulates expression of BAG-neuron genes? We systematically analyzed the cell fate of CO_2-chemosensitive BAG neurons in mutants for each ETS transcription factor. In wild-type animals, $Prom_{flp-19}::gfp$ is expressed by the two BAG neurons, and also by five other paired neurons [19] (Fig. 1 B,C). We found that nine ETS-gene mutants expressed the $Prom_{flp-19}::gfp$ reporter in BAG neurons. *ets-5* mutants, however, failed to express $Prom_{flp-19}::gfp$ in BAG neurons (Fig. 1B,C). Two independent *ets-5* alleles caused the same defect in BAG neuron expression, and a fosmid containing the genomic *ets-5* locus complemented this defect. (Fig. 1C and Fig. S2).

These results confirm the recently reported role for ETS-5 in BAG neuron development [18]. We noted, however, an additional role for ETS-5 in the specification of AWA sensory neurons, which failed to express a $Prom_{flp-19}::gfp$ reporter transgene in *ets-5* mutants (Fig. 1B,C). A previous report indicated that *ets-5* is specifically expressed by the BAG neurons and suggested that ETS-5 functions only to specify BAG neurons but not other sensory neurons [18]. We determined the gene structure of *ets-5* by cloning an *ets-5* cDNA (Fig. S3), and we made an *ets-5::gfp* translational reporter transgene by inserting GFP coding sequences into the last exon of the *ets-5* genomic locus. We observed consistent expression of ETS-5::GFP in the nuclei of BAG neurons and fourteen other neuronal nuclei, including amphid neurons likely to be AWAs (Fig. 2). ETS-5 is therefore required for specification of BAG neurons, but neither its expression nor its function is restricted to BAG neurons.

ETS-5 is required for sensory transduction in CO₂-sensing BAG neurons

ets-5 mutants are defective in an acute CO_2 avoidance behavior [18], which we also observed (Fig. 3A). We monitored the locomotory behavior of animals exposed to a plume CO_2-enriched artificial atmosphere and measured CO_2-evoked reversals. The frequency of reversals by wild-type animals increased dramatically upon presentation of a CO_2 stimulus (Fig. 3A). By contrast, the reversal frequency of animals carrying a caspase-expression transgene that specifically kills BAG neurons did not significantly change in response to presentation of a CO_2 stimulus (Fig. 3A.) Like BAG-ablated animals, the reversal frequency of *ets-5* mutants did not significantly increase in response to a CO_2 stimulus (Fig. 3A). The CO_2-avoidance defect of *ets-5* mutants was complemented by the *ets-5::gfp* transgene used to determine its cellular expression pattern (Fig. 3A). *ets-5* is therefore necessary for acute CO_2 avoidance, a behavior that is driven specifically by BAG neurons. The effect of CO_2 on reversal frequencies of the different strains was calculated as an avoidance index, showing that BAG-ablated animals and *ets-5* mutants were comparably insensitive to CO_2 (Fig. 3B).
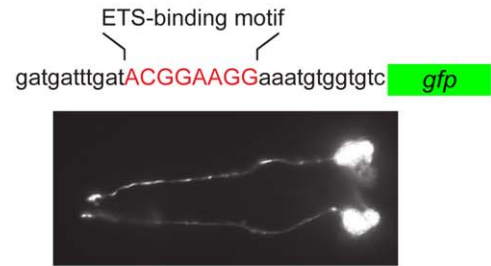
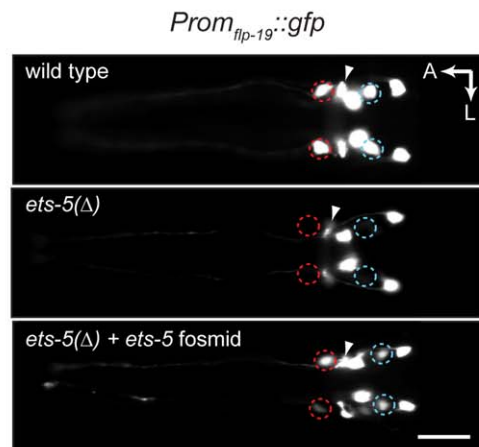| genotype	🟢🟢	⚪⚪	N
wild type	100		50
ets-5(tm1734)		100	50
ast-1(hd1)	100		35
C50A2.4(tm440)	100		26
lin-1(e1777)	100 #		30
C52B9.2(tm413)	100		35
F19F10.1(tm456)	100		31
C24A1.2(tm801)	96	4	25
F19F10.5(ok888)	95	5	42
ets-4(ok165)	100		29
tag-97(ok286)	100		27

Figure 1. An ETS-family transcription factor is required for the specification of *C. elegans* CO₂-chemosensitive BAG neurons. (A) A 31 basepair DNA element comprising a single ETS-binding motif (top) drives expression of GFP specifically in the BAG chemosensitive neurons (bottom). (B) One of ten ETS-family transcription factors encoded by the *C. elegans* genome is required for specification of BAG neurons. Shown is percent of animals mutant for each of ten ETS-family transcription factors encoded by the *C. elegans* genome that are BAGL/R ON (green circles) and BAGL/R OFF (open circles) for expression of a $Prom_{flp-19}::gfp$ reporter transgene. N = number of animals scored. # We found one *lin-1(e1777)* mutant in which $Prom_{flp-19}::gfp$ was not expressed in BAGR. (C) Fluorescence micrographs of $Prom_{flp-19}::gfp$ expression in a wild-type animal, an *ets-5* mutant and an *ets-5* mutant carrying a wild-type copy of the *ets-5* locus in a fosmid-derived transgene. BAGL/R neuron positions are marked by red circles and cells previously identified as AWAL/R [19] are marked by blue circles. The nerve ring is indicated by an arrowhead. The scale bar in lower panel is 20 μm. A: anterior, L: left. The *ets-5* mutant allele was *tm1734*. The $Prom_{flp-19}::gfp$ transgene was *ynIs34* and the *ets-5* rescuing transgene was *rpEx246*.

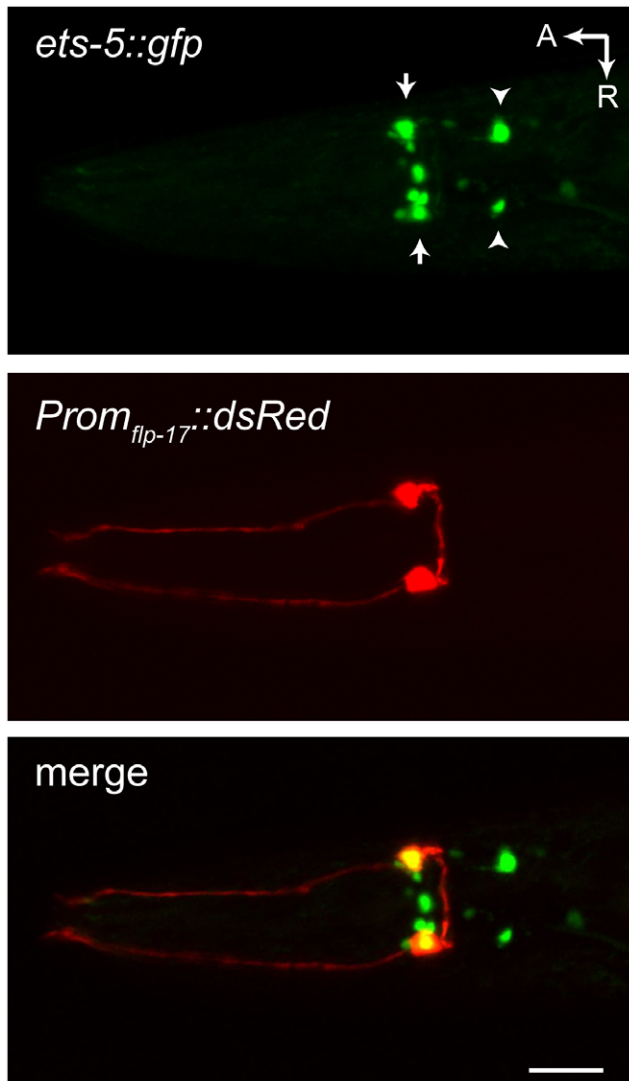doi:10.1371/journal.pone.0034014.g001

Figure 2. ETS-5 is expressed by a subset of head neurons, including the chemosensitive BAG neurons. Ventral view of an adult hermaphrodite expressing an *ets-5::gfp* translational reporter transgene. BAG neurons, which express a Prom$_{flp-17}$::dsRed reporter, are indicated with arrows. Amphid neurons likely to be AWA neurons are indicated by arrowheads. A: anterior, R: right, the scale bar in lower panel is 20 µm. The *ets-5::gfp* transgene is *wzIs80* and the Prom$_{flp-17}$::dsRed transgene is *wzEx36*.
doi:10.1371/journal.pone.0034014.g002

To determine the effect of *ets-5* mutation on the physiology of BAG neurons, we used the ratiometric calcium indicator cameleon YC3.60 [20] to monitor the responses of wild-type and mutant BAG neurons to CO₂ stimuli. Wild-type BAG neurons showed robust responses to CO₂ stimuli; the mean fractional change in the ratio of YFP to CFP emissions to a 10% CO₂ stimulus was greater than 80% (Fig. 3C). By contrast, *ets-5* mutant BAG neurons showed fractional ratio changes of less than 10% in response to the same CO₂ stimulus (Fig. 3D). The BAG neurons of *ets-5* mutants are, therefore, defective in sensory transduction at a point upstream of the generation of an intracellular calcium transient. We next tested whether the transduction defect of *ets-5*-mutant BAG neurons might be caused by defects in the regulation of components of the CO₂-transduction pathway.

ETS-5 directly regulates the receptor-type guanylate cyclase gene *gcy-9*

The receptor-type cyclase GCY-9 is a critical component of the CO₂ transduction pathway (17), and a Prom$_{gcy-9}$::gfp reporter transgene is not properly expressed by *ets-5* mutants (Fig. 4A). Does ETS-5 directly regulate *gcy-9*? We first sought to identify sequences in the *gcy-9* promoter that are required for expression by BAG neurons of a Prom$_{gcy-9}$::gfp reporter. We noted that the ETS domain of ETS-5 is highly similar to the ETS domain of the vertebrate transcription factor Pet1 (Fig. 4B), which functions in the specification of neurons in the vertebrate midbrain [21,22,23]. Pet1 preferentially binds to a consensus sequence AC-CGGAAGTA [24], and the *gcy-9* promoter contains a sequence that is almost identical to the reverse complement of this consensus sequence (Fig. 4C). Moreover, this putative ETS-binding site is highly conserved among nematode species, suggesting that it is functionally important (Figure 4C). This highly conserved ETS-site is adjacent to another putative ETS-binding site. We tested whether these presumptive ETS-binding sites are necessary for *gcy-9* promoter function by introducing into the *gcy-9* promoter a small deletion that removes them. We did not observe any activity of the mutant promoter in BAG neurons (Fig. 4D). We also introduced mutations in both ETS motifs, leaving the rest of the promoter intact. Like the deletion, these mutations abrogated expression of the reporter transgene, indicating that this motif is necessary for *gcy-9* promoter function.

We next tested whether ETS-5 associates *in vivo* with the *gcy-9* promoter at the ETS sites using chromatin immunoprecipitation. ETS-5::GFP immunoprecipitates were enriched for sequences containing the ETS binding site from the *gcy-9* promoter in comparison to precipitates prepared from extracts of non-transgenic animals, which did not express ETS-5::GFP (Fig. 5A). By contrast, sequences upstream of the ETS site were not significantly enriched in ETS-5::GFP immunoprecipitates. ETS-5, therefore, associates with a highly conserved and functionally important sequence element in the *gcy-9* promoter. To determine whether ETS-5 directly interacts with this element, we performed electrophoretic mobility shift assays (EMSAs) using a synthetic 45 base-pair DNA duplex containing the ETS binding site and recombinant ETS-5 protein (Fig. 5B). Recombinant ETS-5 altered the mobility of the duplex, and incorporation of labeled duplex into the complex was efficiently blocked by an excess of unlabeled duplex but not by sequence-scrambled duplex (Fig. 5B). Taken together with the observation that these ETS-binding motifs are required for the function of the *gcy-9* promoter (Fig. 4D), these data indicate that a direct interaction between ETS-5 and sequences in the *gcy-9* promoter is required for expression of *gcy-9* in BAG neurons.

Expression of *gcy-9* bypasses a requirement for *ets-5* in CO₂-avoidance

Are *ets-5* mutants defective in CO₂ sensing principally because they fail to express *gcy-9*, or is *gcy-9* one of many BAG-cell-specific genes that are regulated by ETS-5 and necessary for CO₂ chemosensation? To answer this question, we used promoters that are not regulated by ETS-5 to express *gcy-9* in neurons that (1) mediate an acute avoidance behavior similar to that triggered by BAG neurons and (2) like BAG neurons, use cGMP signaling. The *gcy-36* promoter is active in the URX oxygen-sensing neurons [25], which drive reversals in response to a hyperoxic stimulus [11]. The *gcy-18* promoter is specifically active in thermosensory AFD neurons [26], which also drive reversals [27]. Activity of neither the *gcy-18* nor the *gcy-36* promoter was affected by *ets-5*
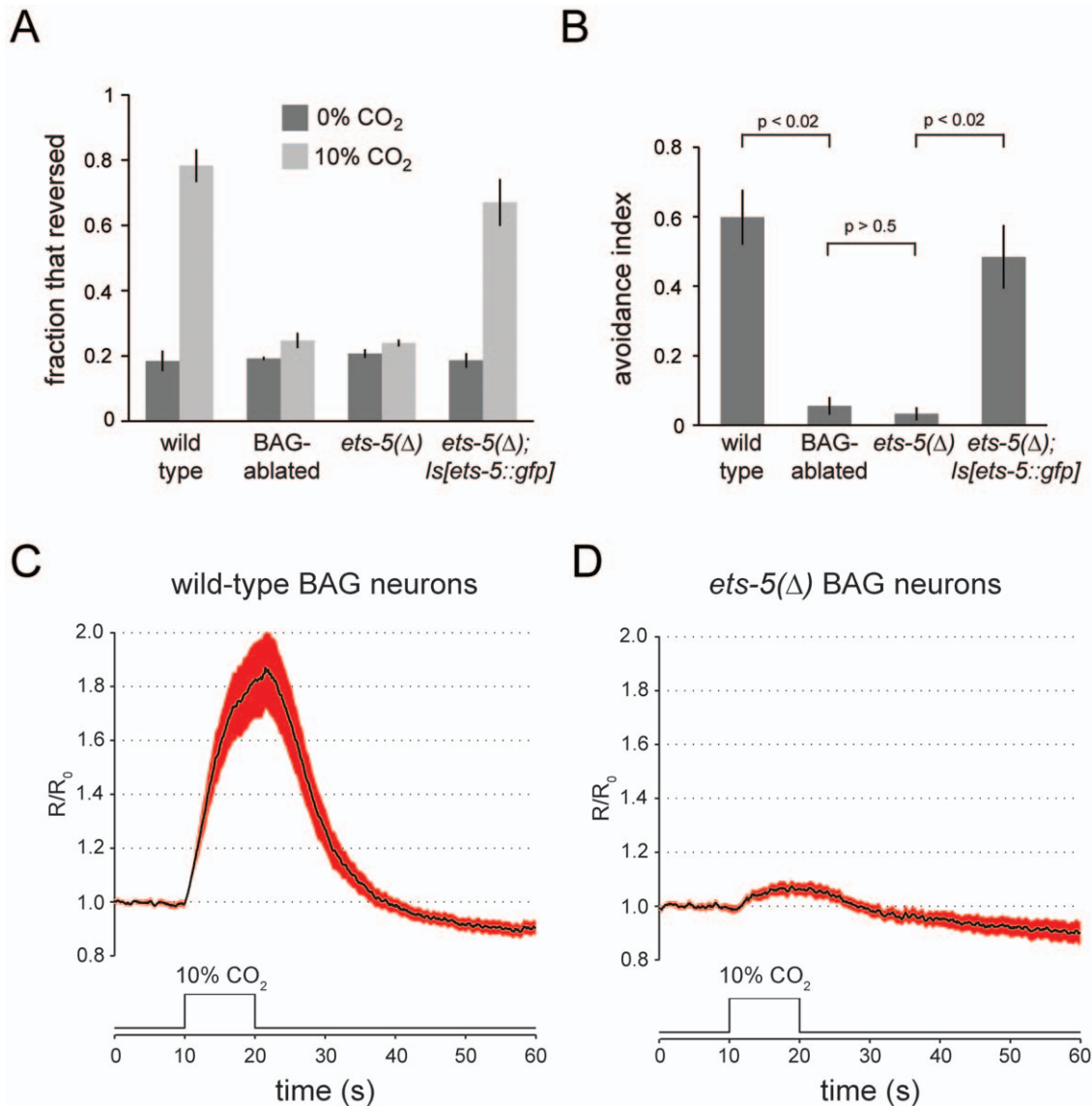
Figure 3. The BAG neurons of *ets-5* mutants are defective in sensory transduction. (A) *ets-5* mutants are defective in a BAG-neuron-dependent CO$_2$ avoidance behavior. Plotted are the mean fractions of animals $\pm$ SEM that reversed during a four second exposure to either control atmosphere (0% CO$_2$, 20% O$_2$, balance N$_2$) or CO$_2$-enriched atmosphere (10% CO$_2$, 20% O$_2$, balance N$_2$). Strains tested were: the wild-type strain N2, the BAG-ablated strain CX11697, the *ets-5* mutant strain FX1734, which carries the *tm1734* deletion allele of *ets-5*, and a derivative of FX1734 that carries the *ets-5::gfp* transgene *wzIs80*. N = 3–5 populations of 30–50 animals. (B) The effect of *ets-5* mutation on CO$_2$ avoidance behavior is comparable to that of BAG neuron ablation. An avoidance index was calculated by subtracting the fraction of animals in a population that reversed in response to control atmosphere from the fraction that reversed in response to CO$_2$-enriched atmosphere. Plotted are the mean avoidance indices for each of the four strains tested $\pm$ SEM. P values were calculated by one-way ANOVA. N = 3–5 populations of 30–50 animals. (C) Wild-type BAG neurons show robust calcium responses to a CO$_2$ stimulus. Wild-type animals carrying a *Prom$_{gcy-9}$::cameleon* transgene, which drives expression of cameleon specifically in BAG neurons, were immobilized and exposed to a 10 s pulse of 10% CO$_2$. Plotted is the mean fractional ratio change in YFP/CFP emissions. The shaded area represents S.E.M. The cameleon expression transgene used was *wzIs82*. (D) The BAG neurons of *ets-5* mutants show reduced calcium responses to a CO$_2$ stimulus. Animals carrying a variant *Prom$_{gcy-33}$::cameleon* transgene, which drives *ets-5*-independent expression of cameleon in BAG neurons, were immobilized and exposed to a 10 s pulse of 10% CO$_2$. Plotted is the mean fractional ratio change in YFP/CFP emissions. The shaded area represents S.E.M. The cameleon expression transgene used was *wzEx56*.
doi:10.1371/journal.pone.0034014.g003

mutation (Fig. 6A). We then tested whether these promoters driving expression of *gcy-9* could rescue the CO$_2$ avoidance defect of *ets-5* mutants. Unlike non-transgenic *ets-5* mutants, which failed to increase reversal frequency in response to a CO$_2$ stimulus, *ets-5* mutants carrying either a *Prom$_{gcy-36}$::gcy-9* transgene or a *Prom$_{gcy-18}$::gcy-9* transgene showed robust avoidance responses to CO$_2$ (Fig. 6B). A requirement for *ets-5* in CO$_2$-avoidance behavior

can therefore be bypassed by expressing the ETS-5 target gene *gcy-9* in neurons that are specified by *ets-5*-independent mechanisms.

Are URX and AFD neurons expressing the ETS-5 target gene *gcy-9* now CO$_2$ chemosensors? We monitored the activity of wild-type and *gcy-9*-expressing URX and AFD neurons using *in vivo* calcium imaging. Wild-type URX neurons showed small decreases in cell calcium in response to a CO$_2$ stimulus. By contrast, URX neurons of transgenic animals showed calcium increases that were
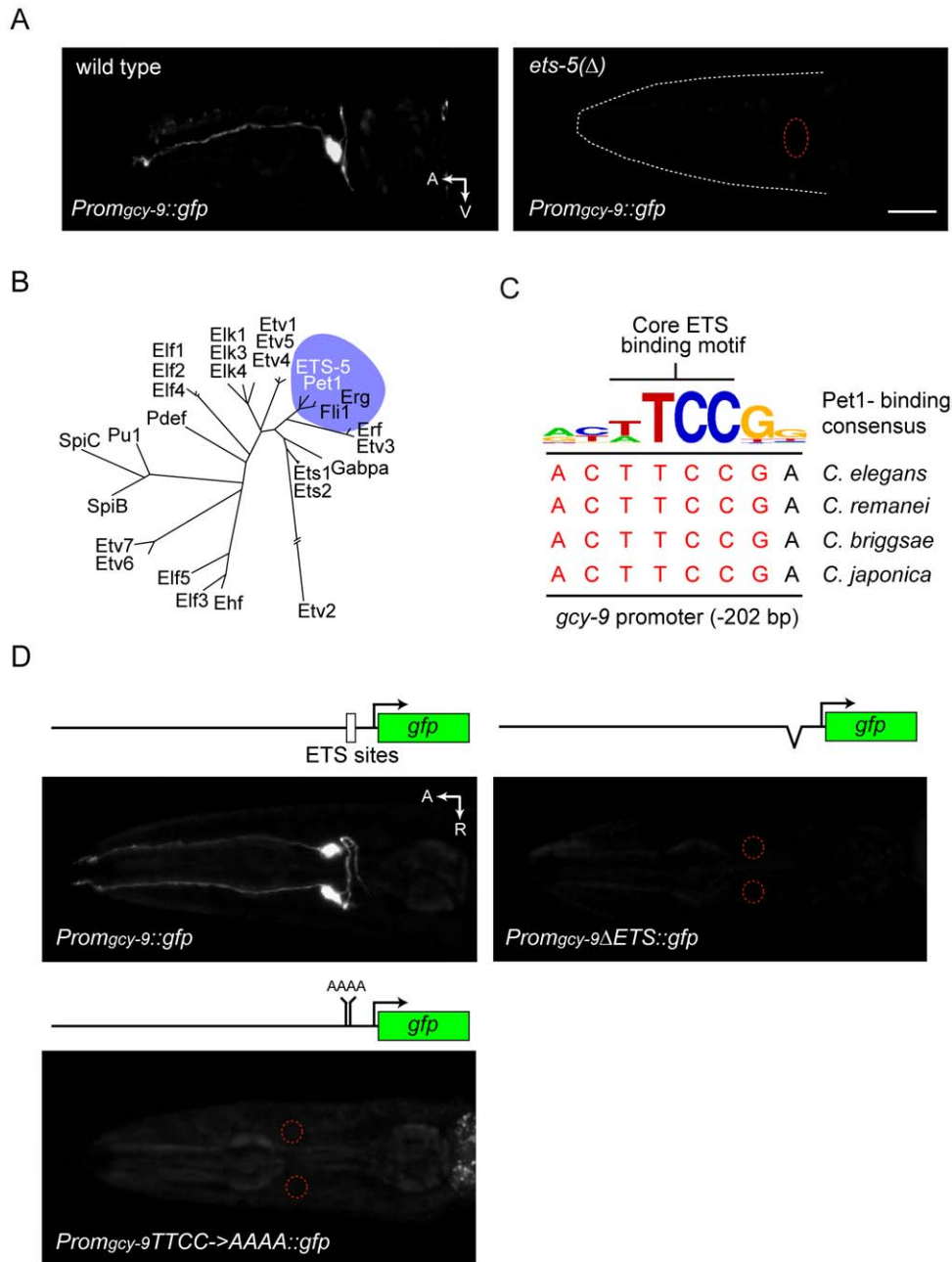
Figure 4. ETS-binding sites in the *gcy-9* promoter are required for its BAG-neuron expression. (A) Fluorescence micrographs of Prom$_{gcy-9}$::gfp expression in a wild-type animal and an *ets-5* mutant. Prom$_{gcy-9}$::gfp expression was principally in BAG neurons (top panel) and was lost in the *ets-5* mutant (bottom panel). In the lower panel, the BAGL neuron position is marked by a red circle. The scale bar in lower panel is 20 μm. A: anterior, V: ventral. The *ets-5* mutant allele was *tm1734*. The Prom$_{gcy-9}$::gfp transgene was *wzEx37*. (B) The ETS domain of ETS-5 is most similar to that of mammalian Pet1. The ETS domains of ETS-5 and 26 mammalian ETS-family transcription factors were identified using the SMART database. Sequences were aligned using the CLUSTALW algorithm and sequence distances were plotted as a dendrogram using the Phylip sequence analysis package. (C) The *gcy-9* promoter contains an evolutionarily conserved ETS-binding motif that is highly similar to the Pet1-binding consensus. A logo of the Pet1-binding consensus sequence [24] is shown aligned to sequences approximately 200 bp upstream of *gcy-9* coding sequences from *C. elegans* and three other rhabditid nematodes. (D) ETS binding motifs in the *gcy-9* promoter are required for promoter function. Shown are ventral views of adult hermaphrodites carrying a 1.9 kb fragment of the *gcy-9* promoter fused to *gfp* coding sequences, or a promoter variant that either carries an 88 bp deletion centered around the ETS binding site at −202 bp, or a variant that carries four-base substitutions in the ETS-binding sites. In each case two lines were tested for GFP expression. Red circles indicate the location of BAG neurons in the animal carrying the mutant transgene. The wild-type *gcy-9* promoter transgene used was *wzEx37* and the mutant promoter transgene was *wzEx38*.
doi:10.1371/journal.pone.0034014.g004

phase-locked to the CO$_2$ stimulus (Fig. 6C). We performed the same measurements on wild-type and transgenic AFD thermosensory neurons (Fig. 6D). Under some experimental conditions,

AFD neurons demonstrate a calcium response to the falling edge of a CO$_2$ pulse [14] *i.e.* an 'off' response. Under our experimental conditions, wild-type AFD neurons showed little response to CO$_2$
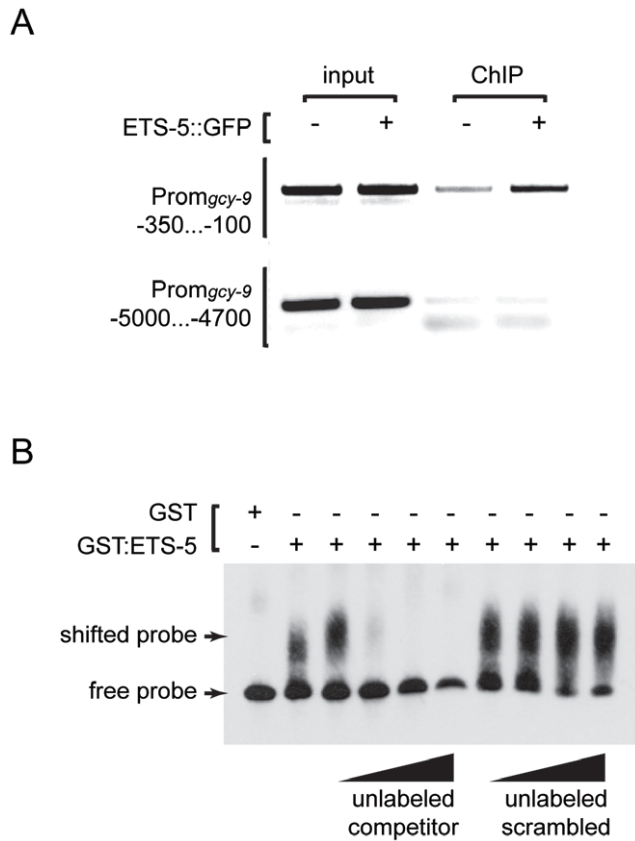
A

B

Figure 5. ETS-5 directly interacts with the *gcy-9* promoter. (A) ETS-5::GFP associates with the *gcy-9* promoter *in vivo*. Anti-GFP immunoprecipitates were prepared from cross-linked extracts of wild-type animals or animals carrying a functional *ets-5::gfp* transgene and interrogated for the presence of *gcy-9* promoter sequences by PCR. Immunoprecipitates from transgenic animals were enriched for *gcy-9* promoter sequences that contained the ETS-binding site at −202 bp. Control sequences at −5000 bp were not enriched in immunoprecipitates from transgenic animals. The *ets-5::gfp* transgene used was *wzIs80*. (B) ETS-5 binds to *gcy-9* promoter sequences *in vitro*. A mobility shift assay was performed with recombinant GST::ETS-5 and a 45 bp biotinylated DNA duplex probe containing the ETS-binding site from the *gcy-9* promoter. Recombinant GST::ETS-5 but not GST alone altered the electrophoretic mobility of the probe. The interaction between GST::ETS-5 and the probe was blocked by a molar excess of unlabeled probe but not by an excess of scrambled probe with the same nucleotide composition. Excess unlabeled wild-type and scrambled competitor probe was added in the following molar ratios: 10×, 50×, 100×, 500×.
doi:10.1371/journal.pone.0034014.g005

stimuli (Fig. 6D). Transgenic AFD neurons expressing *gcy-9*, however, showed robust calcium responses to CO$_2$ stimuli (Fig. 4D), demonstrating that expression of *gcy-9* in AFDs rendered them sensitive to CO$_2$. Expression of the ETS-5 target gene, *gcy-9* is therefore sufficient to confer CO$_2$ chemosensitivity upon neurons that do not normally respond to CO$_2$.

Discussion

Together, our data suggest that the mechanism by which ETS-5 determines CO$_2$-sensitivity is to drive the expression of the receptor-type guanylate cyclase GCY-9, which likely functions as a receptor either for CO$_2$ or for a CO$_2$ metabolite such as bicarbonate or free protons. We previously showed that BAG neuron activation by CO$_2$ requires cyclic-nucleotide-gated ion

channels [17], suggesting that CO$_2$-sensing by BAG neurons minimally requires a two-component transduction pathway: a CO$_2$-activated guanylate cyclase and a cGMP-gated ion channel. Could such a transduction pathway exist in other species? Mammalian genomes encode receptor-type cyclases related to GCY-9. These cyclases have been matched to diverse ligands [28] and are also known to be regulated by interactions with anions, including chloride [29] and bicarbonate [30,31,32,33]. Because vertebrate cyclases are modulated by the CO$_2$ metabolite bicarbonate, this mechanism of cyclase activation might lie at the heart of an evolutionarily conserved pathway for CO$_2$ detection.

Our data show that *gcy-9* expression is a determinant of whether a *C. elegans* neuron is CO$_2$-chemosensitive. How is expression of *gcy-9* restricted to the BAG chemosensors? ETS-5 is necessary for expression of *gcy-9* but is also expressed by neurons that do not express *gcy-9* (Fig. 2). ETS-5 must therefore cooperate with additional, cell-type-specific factors to permit the activation of the *gcy-9* promoter specifically in BAG neurons. For example, overlapping expression of ETS-5 and a co-regulatory partner only in BAG neurons might drive cell-type-specific expression of GCY-9. Similar context-dependent neuronal specification events are known to require such 'combinatorial coding' [34]. Indeed, in other contexts, ETS-family transcription factors interact with co-regulatory transcription factors, including LIM-domain, homeo-domain and JUN proteins [35,36,37]. Further studies will identify ETS-5 interacting partners that specifically drive expression of *gcy-9* in BAG neurons and consequently determine their CO$_2$-chemosensitivity.

ETS-5 has the same domain structure as the vertebrate ETS protein Pet1, and its ETS domain, which mediates sequence-specific interactions with DNA [38], is almost identical to that of Pet1. Like ETS-5, Pet1 functions in the specification of neuronal cell fates [23]. Notably, among the neurons that are specified by Pet1 are serotonergic neurons, that are directly activated by CO$_2$ and have recently been shown to function *in vivo* in the respiratory CO$_2$ chemoreflex [21,22]. In addition to promoting a serotonergic identity, Pet1, like ETS-5, might regulate the expression of genes that constitute a molecular pathway dedicated to the detection of CO$_2$.

Materials and Methods

Strains used in this study

Strains used in this study are listed in Table S1. Strains were grown on NGM agar at 25°C on *Escherichia coli* OP50 except when used for chromatin immunoprecipitation experiments (see below). Transgenic animals were created according to Mello *et al.* [39]. Prom$_{myo-2}$::dsRed coinjection marker was used at 5 ng ul^{-1}. Prom$_{myo-3}$::dsRed was used at 25 ng ul^{-1}. Prom$_{unc-122}$::dsRed was used at 30 ng ul^{-1}. The *lin-15* rescuing plasmid pL15EK was used at 30 ng ul^{-1}. Prom$_{elt-2}$::gfp was used at 3 ng ul^{-1}. rol-6 was used at 100 ng ul^{-1}. GFP, cameleon, dsRed and GCY-9 expression plasmids were injected at 100 ng ul^{-1}. In some cases, extrachromosomal transgenes were integrated using gamma radiation (5000 rads).

Plasmids

A complete list of plasmids used in this study is in Table S2.

Microscopy

Young adults were anaesthetized with 30 mM sodium azide and mounted on a 2% agarose pad made in M9 medium. Series of confocal images were obtained with a Zeiss LSM510 microscope
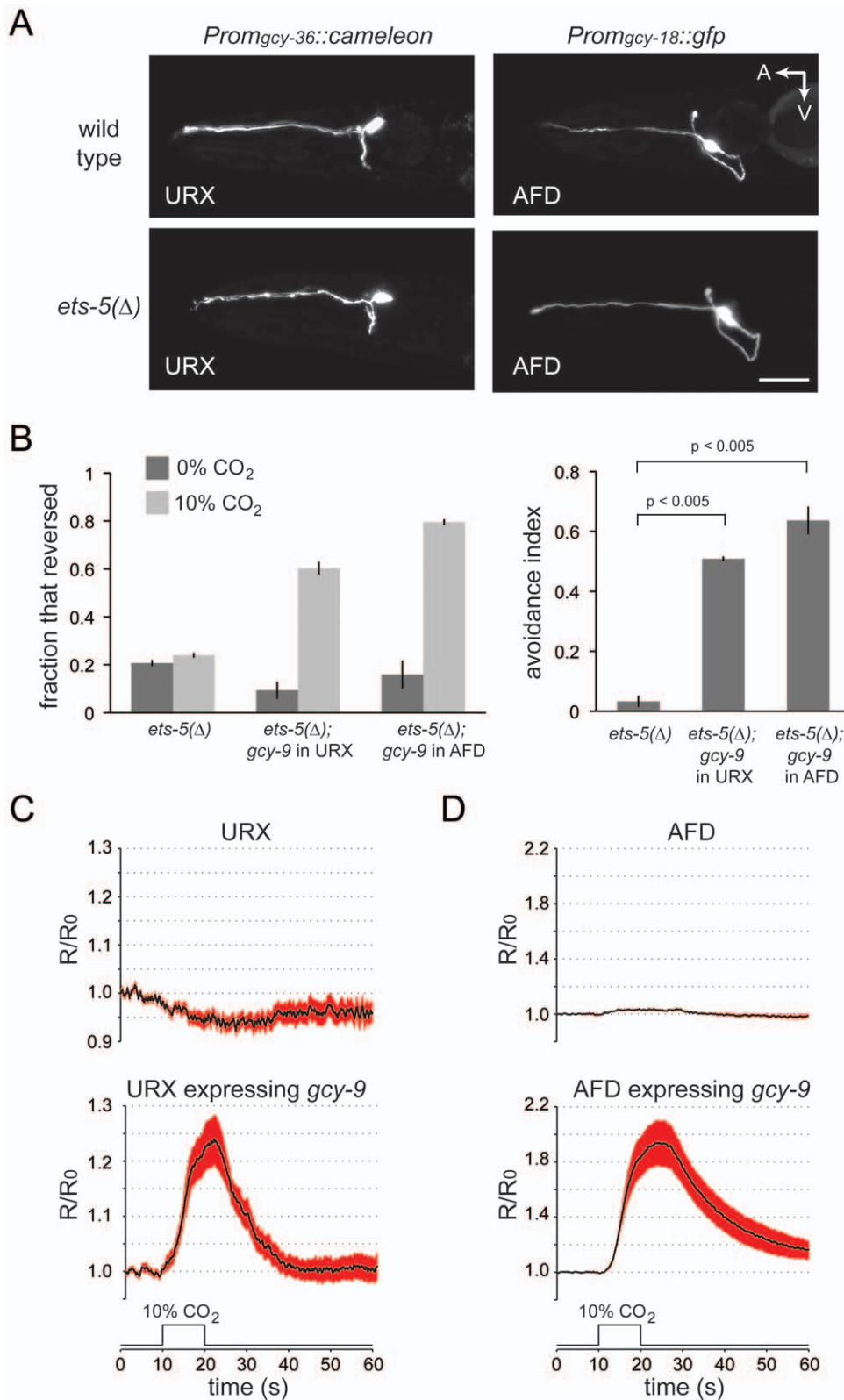
Figure 6. Expression of the ETS-5 target gene *gcy-9* restores CO₂-chemosensitivity to *ets-5* mutants. (A) *gcy-36* and *gcy-18* promoters, which are active in oxygen-sensing and thermosensory neurons, respectively, are not regulated by ETS-5. Shown are lateral views of wild-type and *ets-5* mutant animals carrying either a *gcy-36* reporter, which is expressed by the oxygen-sensing URX neurons, or a *gcy-18* reporter, which is expressed by the thermosensory AFD neurons. A: anterior, V: ventral, scale bar is 20 μm. The Prom$_{gcy-36}$::*cameleon* transgene used was *wzEx39* and the Prom$_{gcy-18}$::*gfp* transgene was *wzEx40*. (B) Expression of *gcy-9* in either the URX oxygen sensors or the AFD thermosensors rescues the behavioral defect of *ets-5* mutants. The left plot shows the mean fraction of animals ± SEM that reversed during a four second exposure to either control atmosphere (0% CO₂, 20% O₂, balance N₂) or CO₂-enriched atmosphere (10% CO₂, 20% O₂, balance N₂). The right plot shows the effect of CO₂ on

reversals as measured with an avoidance index, as in Fig. 2C. Plotted are the mean avoidance indices for each of the four strains tested $\pm$ SEM. P values were calculated by one-way ANOVA. $N = 3$–5 populations of 30–50 animals. The ets-5 mutant strain used was FX1734. The $Prom_{gcy-36}$::gcy-9 transgene used was wzIs97 and the $Prom_{gcy-18}$::gcy-9 transgene was wzEx34. (C) Expression of gcy-9 in the URX oxygen sensors confers sensitivity to CO_2. The ratiometric calcium indicator cameleon was expressed in the URX neurons. Wild-type URX neurons (top panel) showed a small decrease in the ratio of YFP:CFP emissions in response to 10 s CO_2 pulses indicating decreases in cell calcium. URX neurons expressing gcy-9 showed increases in cell calcium in response to CO_2 stimuli, with an average ratio change of greater than 20% (lower panel). The cameleon expression transgene used was wzIs96[$Prom_{gcy-32}$::cameleon] and the gcy-9 expression transgene was wzIs97[$Prom_{gcy-36}$::gcy-9]. (D) Expression of gcy-9 in the AFD thermosensors confers sensitivity to CO_2. Calcium responses of wild-type AFD neurons (top panel) and AFD neurons that express gcy-9 (bottom panel) in responses to a 10% CO_2 stimulus. The cameleon expression transgene was fxIs105[$Prom_{gcy-8}$::cameleon], and the $Prom_{gcy-18}$::gcy-9 transgene was wzEx34. For panels C and D, plots are mean YFP/CFP emissions ratios normalized to the pre-stimulus ratio R_0 ($N = 16$–22 animals). Red shaded areas represent SEM.

and maximum-projection images were created using ImageJ (Rasband, W.S., ImageJ, U. S. National Institutes of Health, Bethesda, Maryland, USA, http://imagej.nih.gov/ij/, 1997–2011).

Behavioral Assay for Acute CO₂ Avoidance

Behavioral assays were carried out essentially as described by Hallem and Sternberg [15]. Three or four trials of 30–50 animals were performed for each genotype. Animals were picked onto unseeded 6 cm nematode growth medium (NGM) agar plates. Gases were certified mixes of 20% oxygen with or without 10% CO_2, balance nitrogen (Airgas).

Statistical analysis

Standard errors and P values were calculated using GraphPad Prism analysis software. P values were calculated from a one-way ANOVA analysis of avoidance indexes.

Chromatin immunoprecipitation

FQ237 wzIs80[ets-5::gfp lin-15AB(+)]; lin-15AB(n765) and N2 animals were grown on 10 cm peptone plates seeded with OP50. A mixed-stage culture of animals was repeatedly washed in M9 and harvested by centrifugation. 5 ml pellets of worms were resuspended in an equal volume of PBS+protease inhibitors and flash-frozen in liquid nitrogen. Frozen pellets were stored at $-80°C$ prior to lysis.

To prepare extracts, frozen pellets were pulverized in a CryoCup (BioSpec) and cross-linked for 10 minutes by addition of 1.1% formaldehyde in PBS+PMSF. Formaldehyde was quenched by addition of 2.5 M glycine in PBS for 5 minutes. Cross-linked extracts were then washed in PBS, resuspended in FA buffer+0.1% sarkosyl, and sonicated using a Branson sonifier set to 35% output, 90% duty cycle with 8 sets of 12 pulses. Cross-linked sonicated extracts were then frozen at $-80°C$.

Prior to immunoprecipitation, extracts were thawed on ice. 5 μg of mouse anti-GFP IgG (Roche) was added to cross-linked sonicated extracts, incubated overnight at 4°C, and recovered using protein G agarose beads (Roche). Beads were washed as described by Ercan et al. [40] and immune complexes were eluted in 150 μl of 100 mM glycine pH 2.5. Protein-DNA crosslinks were reversed by incubation with proteinase K (Qiagen) at 65°C overnight. Nucleic acids were recovered using Qiaquick columns and eluted in 40 μl of elution buffer.

gcy-9 promoter sequences were detected in immunoprecipitates using PCR. To detect the ETS site at -202 base pairs we used the primers 5′-GTTGCATTAGACAGTGTCATAG-3′ and 5′-CCGCAAACAGTAACAATTC-3′. To detect control sequences we used primers 5′-CAATGAGCTGTCCTGGCTTC- 3′ and 5′-TCGACATCTTTGACGCTGCTC-3′. 5 μl of sample from the chromatin immunoprecipitation was used as a template for a 30-cycle PCR.

Electrophoretic mobility shift assay

Recombinant GST::ETS-5 was expressed in *E. coli* strain BL21and purified using glutathione sepharose affinity chromatography (GE Healthcare). 1 μg of recombinant ETS-5 or 2 μg of GST was added to each reaction, which contained 0.1 pmol of 3′-biotin-labeled duplex probe. In some reactions, a molar excess of unlabeled competitor duplex (identical or sequence-scrambled) was included. Reactions were incubated at room temperature for 20 minutes and protein-DNA complexes were separated from unbound probe by electrophoresis in a 6% polyacrylamide gel in $0.5\times$ TBE. Nucleic acids were then transferred to a nylon membrane (Amersham, GE Healthcare) and detected using HRP-coupled streptavidin and enhanced chemiluminscence (Pierce Protein Research Products).

The sequence of the biotinylated probe and the unlabeled competitor was:

5′-ATCCACTTCCGATGGGCCCTTCCGGCATGATAA-GAAGTGAGTGGC-3′.

The sequence of the scrambled competitor was:

5′-CTGACCCCGTGTCGCTAATAGACTCAGTTACG-CAAGATGG-3′.

in vivo calcium imaging

Calcium imaging was performed essentially as previously described [17]. Young adults were immobilized with cyanoacrylate veterinary glue (Surgi-Lock; Meridian Animal Health) on a cover glass coated with a 2% agarose pad made with 10 mM HEPES (pH 7.4). The cover glass was affixed to a custom-made air chamber. The specimen was illuminated with 435-nm excitation light and imaged using a $40\times$ Nikon long-working distance objective (0.75 numerical aperture). The emission image was passed through a DV2 image splitter (Photometrics), and the CFP and YFP emission images were projected onto two halves of a cooled CCD camera (Andor). Images were acquired at 10 Hz, with exposure times between 10 and 50 ms. Gas perfusion was controlled by three-way valves (Numatics) driven by a custom-made valve controller unit. Excitation light, image acquisition, and hardware control were performed by the Live Acquisition software package (Till Photonics). Post-acquisition analysis of ratio plots was performed using custom Matlab scripts, which subtracted linear baseline drift from traces and applied a five-frame boxcar filter to the ratio time series. Custom certified gas mixes used for imaging were obtained from Airgas.

Supporting Information

Figure S1 Deletion analysis of the *flp-17* promoter. (A) Genomic locus of the *flp-17* gene with the location of predicted ETS binding sites shown as blue bars. mCherry protein was driven by the promoter elements indicated with black bars and expression in the BAG neurons was scored. The $Prom9_{flp-17}$ is a 138 bp fragment that is sufficient to drive expression of mCherry protein

in the BAG neurons. $N \geq 30$ animals/transgenic line. (B) Dorsal view of $Prom9_{flp-17}::mCherry$ expression in a wild-type animal. BAG neuron positions are marked by red circles. The scale bar is 20 μm.
(TIF)

Figure S2 *ets-5* mutants have defects in expression of multiple BAG-neuron genes. (A) An independently derived allele of *ets-5* has BAG neurons that fail to express a $Prom_{flp-19}::gfp$ transgene. The fraction of transgenic *ets-5(tm866)* and *ets-5(tm1734)* animals that express GFP in BAG neurons is plotted next to the wild type (+) and *ets-5(tm1734)* mutants carrying rescuing transgenes derived from a fosmid that encompasses the *ets-5* locus. $N \geq 30$, # = independent transgenic lines. (B) Dorsal views of $Prom_{flp-13}::gfp$ expression in a wild-type animal and an *ets-5* mutant. $Prom_{flp-13}::gfp$ expression was lost in the *ets-5* mutant (bottom panel). BAG neuron positions are marked by red circles. The scale bar in lower panel is 20 μm. A: anterior, V: ventral. The *ets-5* mutant allele was *tm1734*. The $Prom_{flp-13}::gfp$ transgene was *ynIs37*. (C) Lateral views of $Prom_{flp-17}::gfp$ expression in a wild-type animal and an *ets-5* mutant. $Prom_{flp-17}::gfp$ expression was lost in the *ets-5* mutant (bottom panel). BAG neuron position in the lower panel is marked by a red circle. The scale bar in lower panel is 20 μm. A: anterior, V: ventral. The *ets-5* mutant allele was *tm1734*. The $Prom_{gcy-17}::gfp$ transgene was *ynIs64*. (D) Lateral views of $Prom_{gcy-31}::gfp$ expression in a wild-type animal and an *ets-5* mutant. $Prom_{gcy-31}::gfp$ expression was lost in the *ets-5* mutant (bottom panel). BAG neuron position in the lower panel is marked by a red circle. The scale bar in lower panel is 20 μm. A: anterior, V: ventral. The *ets-5* mutant allele was *tm1734*. The $Prom_{gcy-17}::gfp$ transgene was *ynIs64*.
(TIF)

Figure S3 Characterization of the *ets-5* transcript. (A) Genomic organization of *ets-5* coding sequences as determined by amplification of *ets-5* cDNA using gene-specific and SL1 primers. cDNAs derived from SL1 trans-spliced messages contained 95 bases of 5′ non-coding sequence (white box) and were organized into five exons. Brackets indicate regions deleted by the *tm1734* and *tm866* mutations. (B) Nucleotide sequence of *ets-5* cDNA. The SL1 leader sequence is underlined. Non-coding sequences are lowercase and exons are denoted by text boxes alternately colored blue and green. (C) Predicted amino acid sequence of ETS-5. Sequences of the ETS homology domain are in white text on a black background.
(TIF)

Table S1 Strains used in this study. Strain designations and complete genotypes of all the strains used in this study.
(DOC)

Table S2 Plasmids used in this study. Complete descriptions of plasmids used in this studies and the sequences of primers used for their construction.
(DOC)

Author Contributions

Conceived and designed the experiments: JB VJ LAM RP NR. Performed the experiments: JB SAZ VJ LAM JGP RP NR. Analyzed the data: JB VJ LAM RP NR. Wrote the paper: JB RP NR.

References

1. Spyer KM, Gourine AV (2009) Chemosensory pathways in the brainstem controlling cardiorespiratory activity. Philosophical Transactions of the Royal Society B: Biological Sciences 364: 2603–2610.
2. Kinney HC, Richerson GB, Dymecki SM, Darnall RA, Nattie EE (2009) The brainstem and serotonin in the sudden infant death syndrome. Annual review of pathology 4: 517–550.
3. Amiel J, Laudier B, Attié-Bitach T, Trang H, de Pontual L, et al. (2003) Polyalanine expansion and frameshift mutations of the paired-like homeobox gene PHOX2B in congenital central hypoventilation syndrome. Nat Genet 33: 459–461.
4. Suh GSB, Wong AM, Hergarden AC, Wang JW, Simon AF, et al. (2004) A single population of olfactory sensory neurons mediates an innate avoidance behaviour in Drosophila. Nature 431: 854–859.
5. Guerenstein PG, Hildebrand JG (2008) Roles and effects of environmental carbon dioxide in insect life. Annu Rev Entomol 53: 161–178.
6. Munger SD, Leinders-Zufall T, Mcdougall LM, Cockerham RE, Schmid A, et al. (2010) An Olfactory Subsystem that Detects Carbon Disulfide and Mediates Food-Related Social Learning. Current Biology. pp 1–7.
7. Hu J, Zhong C, Ding C, Chi Q, Walz A, et al. (2007) Detection of near-atmospheric concentrations of CO2 by an olfactory subsystem in the mouse. Science 317: 953–957.
8. Kwon JY, Dahanukar A, Weiss LA, Carlson JR (2007) The molecular basis of CO2 reception in Drosophila. Proc Natl Acad Sci USA 104: 3574–3578.
9. Jones WD, Cayirlioglu P, Kadow IG, Vosshall LB (2007) Two chemosensory receptors together mediate carbon dioxide detection in Drosophila. Nature 445: 86–90.
10. McGrath PT, Rockman MV, Zimmer M, Jang H, Macosko EZ, et al. (2009) Quantitative mapping of a digenic behavioral trait implicates globin variation in C. elegans sensory behaviors. Neuron 61: 692–699.
11. Zimmer M, Gray JM, Pokala N, Chang AJ, Karow DS, et al. (2009) Neurons detect increases and decreases in oxygen levels using distinct guanylate cyclases. Neuron. pp 865–879.
12. Gray JM, Karow DS, Lu H, Chang AJ, Chang JS, et al. (2004) Oxygen sensation and social feeding mediated by a C. elegans guanylate cyclase homologue. Nature 430: 317–322.
13. Persson A, Gross E, Laurent P, Busch KE, Bretes H, et al. (2009) Natural variation in a neural globin tunes oxygen sensing in wild Caenorhabditis elegans. Nature 458: 1030–1033.
14. Bretscher AJ, Busch KE, de Bono M (2008) A carbon dioxide avoidance behavior is integrated with responses to ambient oxygen and food in Caenorhabditis elegans. Proc Natl Acad Sci USA 105: 8044–8049.
15. Hallem EA, Sternberg PW (2008) Acute carbon dioxide avoidance in Caenorhabditis elegans. Proc Natl Acad Sci USA 105: 8038–8043.
16. Bretscher AJ, Kodama-Namba E, Busch KE, Murphy RJ, Soltesz Z, et al. (2011) Temperature, oxygen, and salt-sensing neurons in C. elegans are carbon dioxide sensors that control avoidance behavior. Neuron 69: 1099–1113.
17. Hallem EA, Spencer WC, McWhirter RD, Zeller G, Henz SR, et al. (2011) Receptor-type guanylate cyclase is required for carbon dioxide sensation by Caenorhabditis elegans. Proc Natl Acad Sci USA 108: 254–259.
18. Guillermin ML, Castelletto ML, Hallem EA (2011) Differentiation of Carbon Dioxide-Sensing Neurons in Caenorhabditis elegans Requires the ETS-5 Transcription Factor. Genetics 189: 1327–1339.
19. Kim K, Li C (2004) Expression and regulation of an FMRFamide-related neuropeptide gene family in Caenorhabditis elegans. J Comp Neurol 475: 540–550.
20. Nagai T, Yamada S, Tominaga T, Ichikawa M, Miyawaki A (2004) Expanded dynamic range of fluorescent indicators for Ca(2+) by circularly permuted yellow fluorescent proteins. Proc Natl Acad Sci USA 101: 10554–10559.
21. Hodges MR, Tattersall GJ, Harris MB, McEvoy SD, Richerson DN, et al. (2008) Defects in breathing and thermoregulation in mice with near-complete absence of central serotonin neurons. J Neurosci 28: 2495–2505.
22. Ray RS, Corcoran AE, Brust RD, Kim JC, Richerson GB, et al. (2011) Impaired Respiratory and Body Temperature Control Upon Acute Serotonergic Neuron Inhibition. Science 333: 637–642.
23. Hendricks TJ, Fyodorov DV, Wegman LJ, Lelutiu NB, Pehek EA, et al. (2003) Pet-1 ETS gene plays a critical role in 5-HT neuron development and is required for normal anxiety-like and aggressive behavior. Neuron 37: 233–247.
24. Wei GH, Badis G, Berger MF, Kivioja T, Palin K, et al. (2010) Genome-wide analysis of ETS-family DNA-binding in vitro and in vivo. EMBO J 29: 2147–2160.

25. Cheung BH, Arellano-Carbajal F, Rybicki I, de Bono M (2004) Soluble guanylate cyclases act in neurons exposed to the body fluid to promote C. elegans aggregation behavior. Curr Biol 14: 1105–1111.

26. Inada H, Ito H, Satterlee J, Sengupta P, Matsumoto K, et al. (2006) Identification of guanylyl cyclases that function in thermosensory neurons of Caenorhabditis elegans. Genetics 172: 2239–2252.

27. Ryu WS, Samuel AD (2002) Thermotaxis in Caenorhabditis elegans analyzed by measuring responses to defined Thermal stimuli. J Neurosci 22: 5727–5733.

28. Wedel B, Garbers D (2001) The guanylyl cyclase family at Y2K. Annu Rev Physiol 63: 215–233.

29. van den Akker F, Zhang X, Miyagi M, Huo X, Misono KS, et al. (2000) Structure of the dimerized hormone-binding domain of a guanylyl-cyclase-coupled receptor. Nature 406: 101–104.

30. Chao Y-C, Cheng C-J, Hsieh H-T, Lin C-C, Chen C-C, et al. (2010) Receptor guanylyl cyclase-G expressed in Grueneberg ganglion olfactory subsystem is activated by bicarbonate. The Biochemical journal.

31. Guo D, Zhang JJ, Huang X-Y (2009) Stimulation of guanylyl cyclase-D by bicarbonate. Biochemistry 48: 4417–4422.

32. Sun L, Wang H, Hu J, Han J, Matsunami H, et al. (2009) Guanylyl cyclase-D in the olfactory CO2 neurons is activated by bicarbonate. Proc Natl Acad Sci USA. pp 2041–2046.

33. Duda T, Sharma RK (2010) Distinct ONE-GC transduction modes and motifs of the odorants: Uroguanylin and CO2. Biochemical and Biophysical Research Communications 391: 1379–1384.

34. Shirasaki R, Pfaff SL (2002) Transcriptional codes and the control of neuronal identity. Annu Rev Neurosci 25: 251–281.

35. Treier M, Bohmann D, Mlodzik M (1995) JUN cooperates with the ETS domain protein pointed to induce photoreceptor R7 fate in the Drosophila eye. Cell 83: 753–760.

36. Yuasa Y, Okabe M, Yoshikawa S, Tabuchi K, Xiong WC, et al. (2003) Drosophila homeodomain protein REPO controls glial differentiation by cooperating with ETS and BTB transcription factors. Development 130: 2419–2428.

37. Guo B, Sallis RE, Greenall A, Petit MM, Jansen E, et al. (2006) The LIM domain protein LPP is a coactivator for the ETS domain transcription factor PEA3. Mol Cell Biol 26: 4529–4538.

38. Karim FD, Urness LD, Thummel CS, Klemsz MJ, McKercher SR, et al. (1990) The ETS-domain: a new DNA-binding motif that recognizes a purine-rich core DNA sequence. Genes Dev 4: 1451–1453.

39. Mello CC, Kramer JM, Stinchcomb D, Ambros V (1991) Efficient gene transfer in C.elegans: extrachromosomal maintenance and integration of transforming sequences. EMBO J 10: 3959–3970.

40. Ercan S, Giresi PG, Whittle CM, Zhang X, Green RD, et al. (2007) X chromosome repression by localization of the C. elegans dosage compensation machinery to sites of transcription initiation. Nat Genet 39: 403–408.